Check for updates

Regulation of divalent metal ions to the aggregation and membrane damage of human islet amyloid polypeptide oligomers†

Yajie Wang, Feihong Meng, Tong Lu, Chunyun Wang and Fei Li [iD] *

The accumulation of human islet amyloid polypeptide (hIAPP) on the surface of pancreatic β cells is closely related to the death of the cells. Divalent metal ions play a significant role in the cytotoxicity of hIAPP. In this study, we examined the roles played by the divalent metal ions of zinc, copper and calcium in the aggregation of both hIAPP18-27 fragment and full-length hIAPP and the ability of their oligomers to damage the membrane of POPC/POPG 4 : 1 LUVs using the ThT fluorescence, TEM, AFM, CD, ANS binding fluorescence and dye leakage experiments. We prepared metal-free and metal-associated oligomers that are similar in size and aggregate slowly using the short peptide and confirmed that the ability of the peptide oligomers to damage the lipid membrane is reduced by the binding to the metal ions, which is closely linked to the reducing hydrophobic exposure of the metal-associated oligomers. The study on the full-length hIAPP showed that the observed membrane damage induced by hIAPP oligomers is either mitigated at a peptide-to-metal ratio of 1 : 0.33 or aggravated at a peptide-to-metal ratio of 1 : 1 in the presence of Zn(II) and Cu(II), while the surface hydrophobicity of hIAPP oligomers was reduced at both peptide-to-metal ratios. The observed results of the membrane damage were attributed to the counteraction between a decrease in the disruptive ability of metal-associated oligomer species and an increase in the quantity of oligomers promoted by the binding of the metal ions to hIAPP oligomers. The former could play a predominant role in reducing the membrane damage at a peptide-to-metal ratio of 1 : 0.33, while the latter could play a predominant role in enhancing the membrane damage at a peptide-to-metal ratio of 1 : 1. This study shows that an enhanced membrane damage could be caused by the oligomer species with a decreased instead of an increased disruptive ability, given that the abundance of the oligomer species is high enough.

Introduction

Human islet amyloid polypeptide (hIAPP) or amylin is composed of 37 amino acid residues.[1–3] It is packaged together with insulin in pancreatic β-cells and co-secreted with insulin out of the cells. Misfolding of hIAPP and resulting amyloid deposit on pancreatic β-cells affect 80% of pancreatic islets in more than 90% of patients with type 2 diabetes mellitus (T2DM).[4–6] Amyloid deposition of other proteins in different tissues is also a key feature of the development of several important neurodegenerative diseases, such as Alzheimer's disease related to Aβ protein and Parkinson's disease related to α-synuclein protein.[7–10] Although the fibrils constructed by β-sheet structure are present in large amounts in the amyloid deposits, small-sized, soluble oligomers formed at the early onset of amyloidosis are proposed to be more cytotoxic and

most likely play a key role in the pathology of T2DM.[11–14] The mechanisms of membrane impairment caused by membrane fragmentation in the fibril growth process of β-sheet rich aggregates,[15,16] and by the formation of transmembrane oligomeric pores[17] were also proposed by *in vitro* study of amylin.

Bio-available divalent metal ions (*e.g.*, zinc and copper) have important effects on the aggregation and cytotoxicity of amylin.[18–20] Islet β-cell granules that store amylin together with insulin contain zinc ion in mM concentration.[21] Zinc ion may affect the aggregation and toxicity of amylin either by binding to the peptide oligomers[22] or by regulating the aggregate state and release of insulin.[23] An alteration in the concentration of zinc ions in the β-cells of the pancreas has been associated with amyloid deposit formation of hIAPP and T2DM.[24,25] The recent discovery of a linkage between T2DM and SLC30A8, a gene encoding zinc transporter ZnT8 specific to β-cells, further suggests that zinc could have an impact on hIAPP toxicity to β-cells.[26–28] Copper is essential for normal cellular function.[29] However, its metabolism is also linked to the progression of T2DM.[30,31] Clinical findings suggest that the patients suffering T2DM have an alteration in copper concentration.[32] A

State Key Laboratory of Supramolecular Structure and Materials, Jilin University, 2699 Qianjin Avenue, Changchun 130012, P. R. China. E-mail: feili@jlu.edu.cn

† Electronic supplementary information (ESI) available. See DOI: 10.1039/d1ra00354b

significant increase in the cytosolic Ca(II) levels was observed in GT1-7 cell lines[33] and β-cells of transgenic mice overexpressing hIAPP.[34] The imbalance of intracellular Ca(II) homeostasis is also correlated with many T2DM-related symptoms.[35,36]

Previous studies *in vitro* have demonstrated that Zn(II) has either a promoting or an inhibiting effect on the fibrillar aggregation and toxicity of hIAPP, depending on their relative concentrations.[37–40] The different effects of Zn(II) ions on T2DM development have also been reported. The activity reducing mutations of ZnT8 are associated with either a decreased[26] or an increased[41] diabetic risk. Cu(II) inhibits hIAPP fibrillation, while the effect of Cu(II) on hIAPP toxicity is controversial. Some studies reported that Cu(II) promotes hIAPP toxicity either by inhibiting hIAPP to form fibrils and inducing hIAPP to form more toxic oligomers,[42,43] or by stimulating the generation of H_2O_2 and β-cell apoptotic induced by hIAPP,[44,45] while other studies demonstrated that Cu(II) has little effect on the cytotoxicity of hIAPP[46] or alleviates the toxicity of hIAPP by inhibiting amylin-evoked oxidative stress in pancreatic cells.[47] His18 residue plays a crucial role in the coordination of Zn(II) and Cu(II) ions with hIAPP. Other residues participating in the coordination of the metal ions with hIAPP are debatable and there is still not a widely-accepted mode.[48] The study about the roles of calcium in the fibrillar aggregation and toxicity of hIAPP are lacking. The results from artificial lipids demonstrated that Ca(II) promotes fibril formation of hIAPP and enhances fragmentation of lipid membrane (POPC/POPS 7 : 3 LUVs) induced by hIAPP fibril elongation, but inhibits membrane damage induced by prefibrillar hIAPP species,[49] and Ca(II) is able to activate a preferential interaction of hIAPP with the hydrophobic core of DPPS membrane.[50]

Despite intensive investigation, our knowledge about the mechanism of divalent metal ions affecting the activity of hIAPP in the impairment of the cellular membrane is still limited. Oligomer intermediates are believed to be toxic species of hIAPP and other amyloid peptides, therefore, the investigation of the effects of metal ions on the features of hIAPP oligomers and on the ability of the oligomers to damage the membrane is significant for understanding the mechanism of hIAPP toxicity. However, the full-length hIAPP has a strong propensity for fibrillation. The oligomers formed by full-length hIAPP are highly unstable and diverse in structure. The binding to the metal ions may change not only the packing structure and stability of hIAPP oligomers, but also the abundance of oligomers (or the proportion of oligomers in total peptide molecules), which impedes a specific characterization of the metal-associated hIAPP oligomers and the comparison between the metal-associated and metal-free oligomer species in some properties, such as the ability to damage the lipid membrane. This means that we could not judge whether the binding to the metal ions increases or decreases the ability of hIAPP oligomer individuals to disrupt the lipid membrane only through the observed disruptive results.

Available evidence suggests that the soluble oligomers impair the cell membrane by a shared characteristic of supramolecular structure, regardless of the amino acid sequences of the peptides/proteins.[51–53] Therefore, the short peptides derived from full-length hIAPP can be used to study the toxic mechanism of the oligomers. Short peptides have a fibrillation rate far slower than full-length peptides and can form the oligomers much more stable than full-length peptides in most instances. If the oligomers with similar sizes are prepared using short peptides in the absence and presence of metal ions, these species of oligomers should not be significantly different in abundance, and thus the aggregation feature and the ability to damage the membrane could be compared between the metal-associated and metal-free oligomer species. The short peptides, such as hIAPP$_{20-29}$ and hIAPP$_{18-27}$, have been used in previous studies of amyloid aggregation and membrane disruption.[54–59] A variety of binding modes of hIAPP–Zn(II) and hIAPP–Cu(II) have been proposed based on the studies of hIAPP fragments, *e.g.*, Ac-IAPP(15–22)–NH$_2$, Ac-IAPP(18–22)–NH$_2$ and its mutants,[60] Ac-PEG–IAPP(14–22)–NH$_2$ (ref. 20) and hIAPP(1–19).[19]

In this work, we intend to elucidate how the binding to Zn(II), Cu(II) and Ca(II) ions affects the ability of hIAPP oligomer individuals to damage the phospholipid membrane and why the metal ions could have an opposite effect (promoting or inhibiting effect) on the hIAPP induced aggregation and membrane damage at different peptide-to-metal stoichiometry. For this purpose, we selected a 10-residue peptide that includes His18 and the amino acid residues in the core region of hIAPP, *i.e.*, hIAPP18-27 (HSSNNFGAIL), as a model peptide, and the phospholipid bilayer composed of POPC/POPG (4 : 1) as model membrane. We prepared the peptide–metal oligomers with similar size distribution and characterized the features of these oligomer species in aggregation and membrane damage using ThT fluorescence, TEM, AFM, CD, ANS binding fluorescence and dye leakage experiments. We also investigated the effects of these metal ions on the aggregation and membrane disruption of full-length hIAPP (KCNTATCATQRLANFLVHSSNNFGAILSSTNVGSNTYNH$_2$ with a disulfide bridge between Cys2 and Cys7) using these experiments. We found that the ability of peptide oligomer individuals to disrupt the lipid membrane is always reduced by the binding to the metal ions, whatever the concentrations of the metal ions are, while the observed membrane damage induced by hIAPP oligomers is either aggravated at a peptide-to-metal ratio of 1 : 1 or alleviated at a peptide-to-metal ratio of 1 : 0.33. We suggest that the observed results of the membrane damage at different peptide-to-metal ratios could originate from a competitive effect between an increase in the abundance of the metal-associated hIAPP oligomer species and a decrease in its disruptive ability.

Results

Morphology and size distribution of 10-peptide oligomers

We prepared four species of oligomers by incubating 1 mM 10-peptide (named as ia10) in 4 °C Milli-Q water for 10 minutes in the absence and presence of Ca(II), Zn(II) or Cu(II) ions at a peptide-to-metal molar ratio of 1 : 1. TEM images showed that all the four species of oligomers are approximately spherical, with a similar diameter distribution ranging from *ca*. 10 nm to *ca*. 30 nm and a mean diameter of *ca*. 19 nm (Fig. 1A and Fig. S1 in ESI†). The size distributions of the oligomers were also
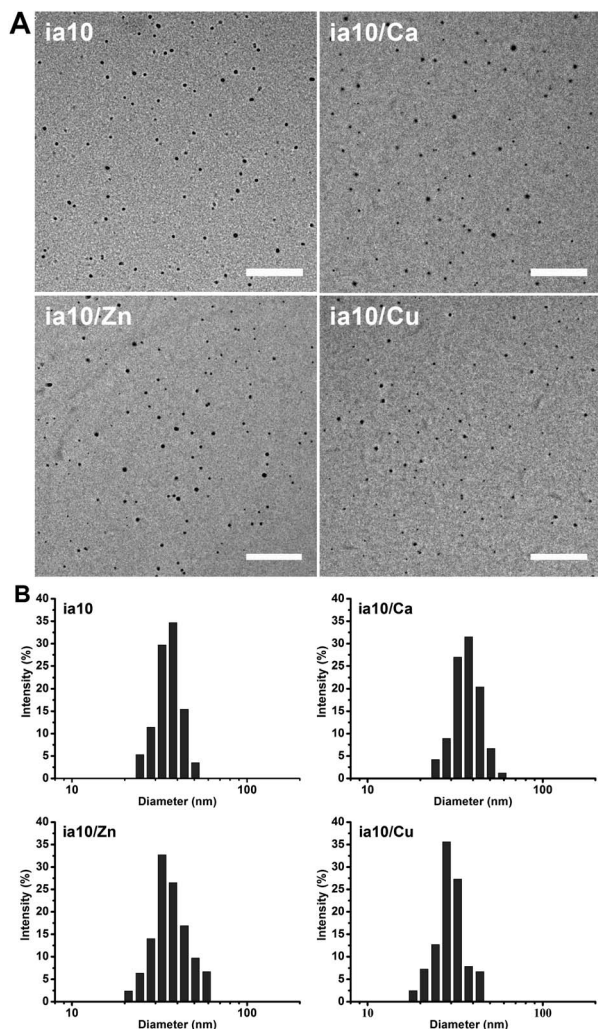
Fig. 1 (A) Morphology of the 10-peptide oligomers obtained by TEM (the scale bars are 500 nm), and (B) size distributions of these oligomers in 4 °C Milli-Q water obtained by DLS.
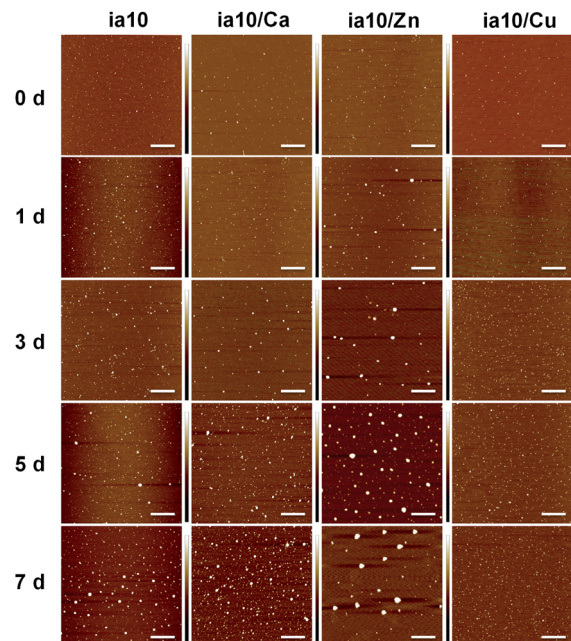

Fig. 2 AFM images of the 10-peptide oligomers recorded at the initial time of incubation (0 d) and after various days of incubation (1–7 d) in phosphate buffer with POPC/POPG 4 : 1 LUVs at pH 7.4. The concentrations of peptide and total lipids were 50 μM and 500 μM, respectively. The scale bars are 1 μm.

promoted by the association with Zn(ɪɪ). The effect of Ca(ɪɪ) on the aggregation of the peptide was small.

The aggregation of the four species of oligomers was also monitored by the CD spectra in the presence of POPC/POPG 4 : 1 LUVs (Fig. 3). The CD spectra of all these oligomers showed a negative molar ellipticity at *ca.* 197 nm at initial time of incubation. With increasing incubation time, the band at *ca.* 197 nm dramatically changed from a stronger negative signal to

obtained by DLS experiments and the hydrodynamic diameters ranging from *ca.* 25 nm to *ca.* 50 nm (with mean diameters of *ca.* 28–38 nm) were obtained (Fig. 1B).

Aggregation of 10-peptide oligomers

The aggregation of the four species of 10-peptide oligomers was monitored by ThT fluorescence assays and AFM measurements. The increase in the ThT fluorescence emission was not observed for all these species of oligomers within 7 days of incubation in phosphate buffer at pH 7.4 in the presence of POPC/POPG 4 : 1 LUVs (Fig. S2 in ESI†). The growth of these oligomers with time was observed in the AFM images (Fig. 2). Although these oligomers grew at different rates, none of them formed fibrils within 7 days of incubation in the presence of lipid membrane. The aggregation rate of the oligomers decreased in an order of ia10/Zn, ia10 and ia10/Ca (the two were indistinguishable), and ia10/Cu. This implies that the aggregation of the 10-peptide oligomers is inhibited by the association with Cu(ɪɪ), but
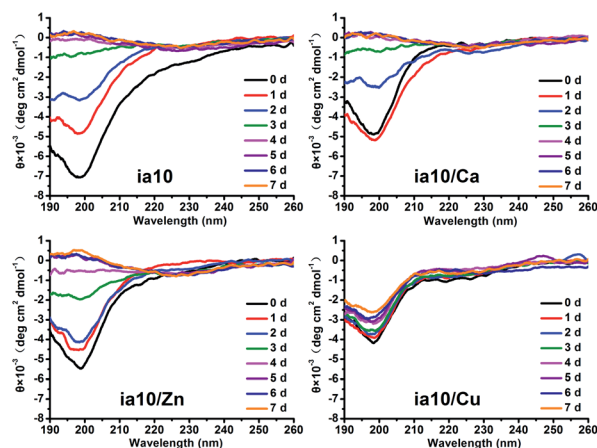

Fig. 3 CD spectra of 10-peptide oligomers recorded at the initial time of incubation (0 d) and after various days of incubation (1–7 d) in phosphate buffer suspended with POPC/POPG 4 : 1 LUVs at pH 7.4. The concentrations of peptide and total lipids were 50 μM and 500 μM, respectively.

a weaker positive signal along with an emergence of a very weak negative signal at *ca.* 225 nm for ia10, ia10/Ca and ia10/Zn oligomers. In contrast, the CD spectrum of ia10/Cu oligomers changed a little. This suggests that the ia10/Cu oligomers could be more stable than other species of oligomers.

The ThT fluorescence assay, AFM and CD measurements were also performed for the four species of 10-peptide oligomers in phosphate buffer at pH 7.4 without lipid vesicles (Fig. S2–S4 in ESI†). The results of ThT fluorescence and AFM were very similar to those obtained in the presence of lipid membrane. The CD spectra obtained in the absence of lipids were similar to those obtained in the presence of the lipid membrane at the initial time of incubation, only with a small extent of increase in the intensity of the negative molar ellipticity at *ca.* 197 nm. Although the change in the intensity of the negative molar ellipticity with time observed in the absence of lipids was evidently smaller than that observed in the presence of lipids, a slower change in the intensity of the negative signal for ia10/Cu oligomers than for other species of oligomers was also observed in the absence of lipids.

Membrane disruption and surface hydrophobicity of 10-peptide oligomers

The release of calcein from POPC/POPG 4 : 1 LUVs was monitored by the leakage assay within 7 days of incubation in the presence of the 10-peptide oligomers (Fig. 4A). The dye leakage percentages reached a plateau on the 5th day for all these species of oligomers. However, the height of the plateau was different for different species of oligomers. A highest leakage

plateau was observed for the oligomers formed in the absence of the metal ions, while the leakage plateau was lowered by the oligomers formed in the presence of the divalent metal ions, and the inhibition effects of the metal ions on the oligomer induced dye leakage increased in an order of Ca(ɪɪ), Zn(ɪɪ) and Cu(ɪɪ). This indicates that the association of the 10-peptide with these metal ions reduces the ability of the resulting oligomers to damage POPC/POPG 4 : 1 LUVs. Of the three divalent metal ions, the effect of Cu(ɪɪ) on the disruptive ability of the oligomer was the largest, and that of Ca(ɪɪ) was the smallest. The dye leakage of the LUVs incubated with just the metal ions was also measured to test for the effect of the metal ions on the LUV permeability (Fig. S5 in ESI†). The leakage amounts induced by the ion themselves were very small and the largest quantity was no more than 5%.

The hydrophobic exposure feature of the oligomers was explored by the fluorescence quenching experiment and the ANS binding fluorescent experiment to understand the difference in the membrane destruction ability of the four species of oligomers. The fluorescence emission of the single phenylalanine at position 6 of the 10-peptide was monitored after the addition of different concentrations of acrylamide (Fig. 4B and S6 in ESI†). The degree of fluorescence quenching by acrylamide decreased in an order of ia10, ia10/Ca, ia10/Zn and ia10/Cu oligomers, with a quenching constant (K_{sv}) of 66, 60, 49 and 42 M^{-1}, respectively. This indicates that the aromatic side chains in the metal-associated oligomers are less water exposed than those in the metal-free oligomers and the surface hydrophobic exposure of the aromatic residues in the metal-associated oligomers decreases in an order of ia10/Ca, ia10/Zn and ia10/Cu. In the ANS binding fluorescence assays, both an increase in intensity and a decrease in wavelength (blue shift) of the ANS fluorescence signals with increasing peptide concentration were observed for all these species of 10-peptide oligomers (Fig. 4C, D, and S7 in ESI†). The changes in the ANS fluorescence spectra reduced in an order of ia10, ia10/Ca, ia10/Zn and ia10/Cu, indicating an decrease in the surface hydrophobicity of the oligomers in this order. The metal ion themselves have no effect on the ANS fluorescence (Fig. S8 in ESI†). The results of ANS binding fluorescence assays were consistent with those of acrylamide fluorescence quenching experiments.
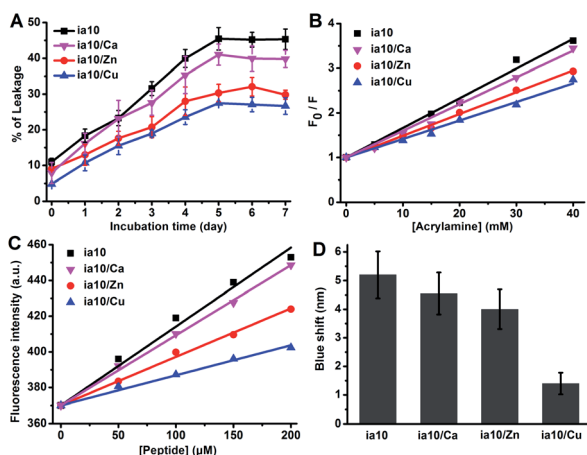
Characterization of hIAPP oligomers preformed in stock solution in the absence and presence of metal ions

We first performed DLS measurements immediately after freeze-dried hIAPP was dissolved in 4 °C Milli-Q water at 1 mM (stock solution) in the absence and presence of metal ions Ca(ɪɪ), Zn(ɪɪ) and Cu(ɪɪ) at peptide-to-metal ratios of 1 : 0.33 (Fig. 5A) and 1 : 1 (Fig. 5B). A distribution of hydrodynamic diameter centered at *ca.* 20 nm was observed for metal-free hIAPP sample. The size distribution of hIAPP sample was little affected by the addition of Ca(ɪɪ), but moved slightly towards the direction of decreasing diameter by the addition of Zn(ɪɪ) and Cu(ɪɪ). This suggests that hIAPP could exist in an equilibrium between monomers and the early oligomers or in a mixture of diverse metastable oligomers initially.[42] The Zn(ɪɪ)- and Cu(ɪɪ)-associated

Fig. 4 (A) Leakage percentage of calcein releasing from POPC/POPG 4 : 1 LUVs upon incubation with the four species of 10-peptide oligomers in phosphate buffer at pH 7.4 for different durations (the concentrations of peptide and total lipids were 50 μM and 500 μM, respectively), (B) phenylalanine fluorescence quenching by acrylamide for the four species of 10-peptide oligomers in 4 °C Milli-Q water at a peptide concentration of 50 μM, (C) fluorescence emission of ANS induced by binding to the four species of oligomers in 4 °C Milli-Q water at varied peptide concentrations and a fixed ANS concentration (300 μM), and (D) the blue shift of ANS fluorescence induced by binding to the peptide oligomers in 4 °C Milli-Q water at a peptide concentration of 200 μM and an ANS concentration of 300 μM.
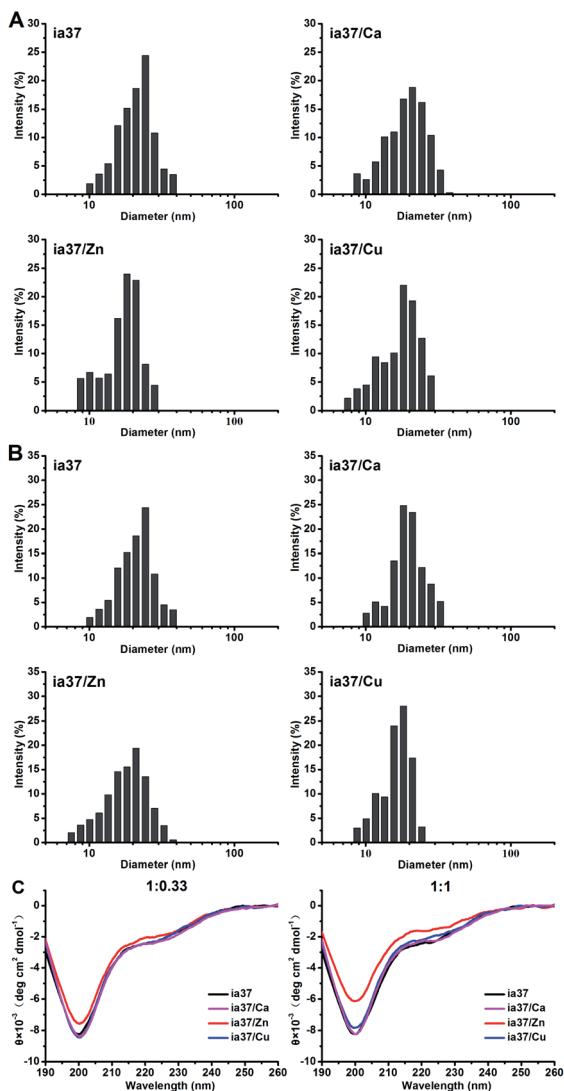
Fig. 5 DLS results of hIAPP oligomers preformed in 4 °C Milli-Q water at a peptide concentration of 1 mM in the absence and presence of Ca(II), Zn(II) and Cu(II) at peptide-to-metal ratios of 1 : 0.33 (A) and 1 : 1 (B), and CD spectra of hIAPP oligomers preformed in 4 °C Milli-Q water in the absence and presence of the metal ions at peptide-to-metal ratios of 1 : 0.33 and 1 : 1 (C). The concentration of peptide was diluted to 5 μM and 15 μM in the DLS and CD measurements, respectively.

Effects of metal ions on the aggregation of hIAPP oligomers

The aggregations of full-length hIAPP with 37 amino acid residues (named as ia37) in the absence and presence of Ca(II), Zn(II) and Cu(II) were investigated at both peptide-to-metal ratios of 1 : 0.33 and 1 : 1. The ThT fluorescence experiments performed in phosphate buffer at pH 7.4 demonstrated that the fibrillar aggregation of hIAPP was little affected by Ca(II) and inhibited by Cu(II) at both peptide-to-metal ratios, while the fibrillation of hIAPP was either inhibited by Zn(II) at a peptide-to-metal ratio of 1 : 0.33 or promoted by Zn(II) at a peptide-to-metal ratio of 1 : 1 (Fig. 6A). In the presence of POPC : POPG 4 : 1 LUVs, the fibril formation of hIAPP was inhibited by both Zn(II) and Cu(II) and the inhibition effect was increased from a peptide-to-metal ratio of 1 : 0.33 to 1 : 1. Cu(II) was more potent than Zn(II) in the inhibition of hIAPP fibrillation (Fig. 6B). Metal ion themselves have no effect on the ThT fluorescence results (Fig. S9†). The results of ThT fluorescence experiments observed in the presence of POPC/POPG 4 : 1 LUVs were confirmed by AFM imaging (Fig. S10 in ESI†).

We recorded the time-dependent CD spectra of hIAPP at peptide-to-metal ratios of 1 : 0.33 and 1 : 1 in the presence of POPC/POPG 4 : 1 LUVs to monitor the changes in the secondary structure of hIAPP (Fig. S11 in ESI†). We found that hIAPP undergoes the structural transfer from initially a random coil dominant structure to finally a β-sheet structure via an α-helix intermediate with a decreasing rate of structural transfer in an order of ia37 and ia37/Ca (both were indistinguishable), ia37/Zn and ia37/Cu at both peptide-to-metal ratios of 1 : 0.33 and 1 : 1, and the difference in the rate of structural transfer is more obvious at peptide-to-metal ratio of 1 : 1.

Effects of metal ions on the surface hydrophobicity of hIAPP oligomers and membrane damage

The damage of POPC/POPG 4 : 1 LUVs induced by hIAPP oligomers with and without the metal ions was examined by leakage

hIAPP oligomers could be a little bit smaller than metal-free and Ca(II)-associated hIAPP oligomers on average.

The structures of hIAPP oligomers preformed in 4 °C Milli-Q water at 1 mM in the absence and presence of Ca(II), Zn(II) and Cu(II) were characterized by CD measurements (Fig. 5C). The results showed that hIAPP adopts an unordered or random coil structure in all these species of oligomers. However, an evident reduction in the intensity of the negative ellipticity at ca. 200 nm was observed in the CD spectra of hIAPP oligomers formed in the presence of Zn(II), while no changes were observed in the spectra of hIAPP oligomers formed in the presence of Cu(II) and Ca(II), compared with the CD spectrum of metal-free hIAPP oligomers. This suggests that the quantity of hIAPP oligomers could be increased by the binding of Zn(II) to the oligomers.
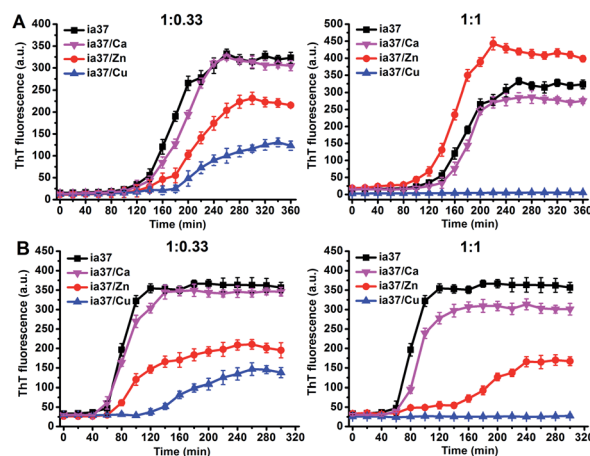

Fig. 6 ThT fluorescence of hIAPP alone and hIAPP mixed with the metal ions at peptide-to-metal ratios of 1 : 0.33 (left) and 1 : 1 (right) in phosphate buffer at pH 7.4 in the absence (A) and presence (B) of POPC/POPG 4 : 1 LUVs. The concentrations of peptide and total lipids were 15 μM and 1.5 mM, respectively.
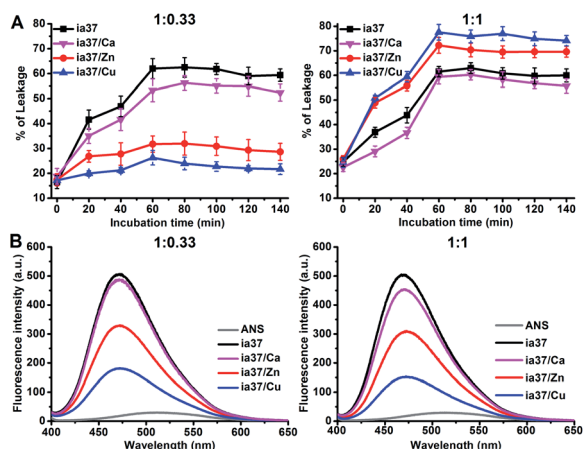
Fig. 7 (A) Percentages of calcein releasing from POPC/POPG 4 : 1 LUVs after different time of incubation with hIAPP in the absence and presence of the metal ions at different peptide-to-metal ratios in phosphate buffer at pH 7.4 (the concentrations of peptide and total lipids were 15 μM and 1.5 mM, respectively), (B) results of ANS binding fluorescence experiments for hIAPP oligomers in 4 °C Milli-Q water without and with the metal ions at different peptide-to-metal ratios (the concentrations of both ANS and peptide were 15 μM).

assays (Fig. 7A). The results showed that the dye leakage percentages induced by hIAPP oligomers formed in the presence of these metal ions at a peptide-to-metal ratio of 1 : 0.33 were less than the leakage caused by metal-free hIAPP oligomers, and the reduction in the dye leakage was more pronounced in the presence of Zn(II) and Cu(II) than that in the presence of Ca(II). In contrast, the mixture of hIAPP with either Zn(II) or Cu(II) at a peptide-to-metal ratio of 1 : 1 resulted in an increase in the dye release compared with the result of hIAPP alone. The effects of Cu(II) on the performance of hIAPP oligomers triggering dye release at both peptide-to-metal ratios were slightly greater than those of Zn(II).

The surface hydrophobicity of hIAPP oligomers in the absence and presence of the metal ions was probed using the ANS binding fluorescence experiments performed in 4 °C Milli-Q water (Fig. 7B). The fluorescence intensity of ANS was enhanced by binding to hIAPP oligomers either with or without the metal ions. However, the ANS fluorescence enhancements observed in the presence of the metal ions were smaller than that observed in the absence of the metal ions and the enhancements decreased in an order of ia37/Ca(II), ia37/Zn(II) and ia37/Cu(II) at both peptide-to-metal ratios of 1 : 0.33 and 1 : 1. This indicates that the surface hydrophobicity of hIAPP oligomers is reduced by the binding to the metal ions, and the role of the metal ions in reducing hydrophobic exposure of hIAPP oligomers increases according to the order of Ca(II), Zn(II) and Cu(II).

Discussion

A growing body of evidence has proposed that small and soluble hIAPP oligomers are the toxic form responsible for the membrane impairment and β-cell death, and the bioavailable

divalent metal ions have a significant role in the amyloidogenic process and toxicity of hIAPP. However, the issue of how the divalent metal ions affect the activity of the oligomers in membrane damage has not been clarified. In this study, we first prepare four species of oligomers composed of hIAPP18-27 peptide alone and the mixtures of the 10-peptide with Ca(II), Zn(II) and Cu(II) ions at a peptide-to-metal molar ratio of 1 : 1. All these 10-peptide oligomers are very similar in size distribution and aggregate very slowly. They do not form fibrils even after 7 days of incubation in either lipid free or liposome (POPC/POPG 4 : 1 LUVs) suspended phosphate buffer at pH 7.4. Therefore, we can compare these different species of oligomers in their ability to disrupt the lipid membrane.

The results of leakage assay show that the damage of the POPC/POPG 4 : 1 LUVs induced by the 10-peptide oligomers is inhibited in the presence of Ca(II), Zn(II) or Cu(II) ions and the inhibition effect of the metal ions increases in an order of Ca(II), Zn(II) and Cu(II). The initial interaction of the oligomers with the membrane may be crucial for their disruptive activity, while the growing of the oligomers and simultaneously occurring change in the secondary structure of peptide could be insignificant. Otherwise, rather different growing rate and structural evolution of Cu(II)-associated oligomers from other three species of oligomers (Fig. 3) could lead to different leakage kinetics, instead of a similar time dependence of dye leakage, as observed in this study (the dye leakage amounts induced by all these four species of oligomers reach a plateau on the 5th day of incubation, Fig. 4A). Previous study reported that both size and surface hydrophobicity are generic determinants of misfolded oligomer cytotoxicity.[61] Our results of TEM and DLS demonstrate that the four species of oligomers are very similar in mean diameter initially, implying that they are not largely different in quantity at the same peptide concentration. Therefore, the observed differences in the percentages of dye leakage induced by these species of oligomers could be related to the differences in the disruptive ability of these species of oligomer individuals. The surface hydrophobicity of the four species of oligomers decreases in an order of ia10, ia10/Ca, ia10/Zn and ia10/Cu, an order consistent with the disruptive ability of the four species of oligomers, suggesting that the disruptive ability of the four species of oligomers are closely correlated with their surface hydrophobicity.[62] A reduction in the surface hydrophobicity of oligomers by the binding to the metal ions could decrease the hydrophobic interaction of the oligomers with the lipid membrane, and in doing so, decrease the membrane damage.[63]

We further investigate the aggregation and membrane disruption of full-length hIAPP peptide in the absence and presence of metal ions Ca(II), Zn(II) and Cu(II). Unlike the short peptide, the full-length hIAPP peptide aggregates and forms fibrils rapidly. We find that the fibril formation of hIAPP in buffer solution at pH 7.4 is inhibited in the presence of Zn(II) at a peptide-to-metal ratio of 1 : 0.33, but promoted at a peptide-to-metal ratio of 1 : 1. Previous study has demonstrated that a single Zn(II) ion preferentially binds to hIAPP oligomers by multiple interactions, which alters the monomer–oligomer equilibrium and promotes the formation of oligomers.[22,42] Although the binding to Zn(II) promotes the formation of hIAPP

oligomers, it restricts the conformational change of hIAPP and thus inhibits the formation of β-sheet structured aggregates/fibrils. At a lower Zn(ɪɪ) concentration (*e.g.*, at a peptide-to-metal ratio of 1 : 0.33), preformed hIAPP oligomers could be largely stabilized by the binding to Zn(ɪɪ), while the quantity of oligomers could not be increased significantly. In this case, the inhibition effect on hIAPP aggregation caused by the restriction of Zn(ɪɪ) to the structural transformation of hIAPP oligomers could overweigh the promotion effect caused by the catalyzation of Zn(ɪɪ) to the formation of hIAPP oligomers, and therefore the fibrillar aggregation of hIAPP is suppressed. With the increase in Zn(ɪɪ) concentration (*e.g.*, at a peptide-to-metal ratio of 1 : 1), the quantity of hIAPP oligomers formed at the early stage of aggregation could be significantly increased compared to that of metal-free hIAPP oligomers.[22] An evident decrease in the intensity of the negative ellipticity at *ca.* 200 nm observed in the CD spectrum of hIAPP/Zn(ɪɪ) mixture at a peptide-to-metal ratio of 1 : 1 (Fig. 5C) could result from the increase in the abundance of hIAPP oligomers promoted by the binding to Zn(ɪɪ). Although the binding of hIAPP oligomers to Zn(ɪɪ) may elevate the energy barrier of hIAPP conformational transformation, a pronounced increase in the quantity of Zn(ɪɪ)-associated hIAPP oligomer species at a peptide-to-metal ratio of 1 : 1 accelerates the fibrillar aggregation of hIAPP in buffer solution (Fig. 6A).

Previous study proposed that a single Cu(ɪɪ) ion could bind to hIAPP monomer in a 3N1O form[64] and this form of coordination could be maintained even in a metal-associated hIAPP oligomers.[42] A higher affinity of Cu(ɪɪ) for hIAPP (K_a: *ca.* 8.9×10^7 M^{-1} for Cu(ɪɪ) and *ca.* 9.1×10^5 M^{-1} for Zn(ɪɪ)[42]) and the distinct coordination property strongly restrict the conformational change of oligomeric hIAPP. Therefore, the fibrillar aggregation of hIAPP in buffer solution is always inhibited in the presence of Cu(ɪɪ) no matter what the peptide-to-metal ratios are.

In the presence of the lipid membrane, however, the fibrillation process of hIAPP is inhibited by the addition of Zn(ɪɪ) and Cu(ɪɪ) at both peptide-to-metal ratios of 1 : 0.33 and 1 : 1. A possible reason for this is that the electrostatic interactions of Zn(ɪɪ)- and Cu(ɪɪ)-associated hIAPP oligomers with the negatively charged lipid membrane are stronger than that of metal-free hIAPP oligomers. Although the aggregations of all the metal-free and metal-associated hIAPP oligomers are accelerated in the presence of the membrane by a local concentration of peptide at the membrane surface, enhanced electrostatic interactions of Zn(ɪɪ)- and Cu(ɪɪ)-associated hIAPP oligomers with the head-groups of the lipid membrane could reduce the peptide–peptide or oligomer–oligomer interactions and therefore decrease the rate of hIAPP fibrillation at the membrane surface, in comparison with metal-free hIAPP oligomers.

Interestingly, whereas the fibrillar aggregation of hIAPP oligomers is inhibited by Zn(ɪɪ) and Cu(ɪɪ) ions in the presence of POPC/POPG 4 : 1 LUVs at both peptide-to-metal ratios of 1 : 0.33 and 1 : 1, the membrane damage caused by Zn(ɪɪ)- and Cu(ɪɪ)-associated hIAPP oligomers is either reduced at a peptide-to-metal ratio of 1 : 0.33 or enhanced at a peptide-to-metal ratio of 1 : 1. However, the surface hydrophobicity of hIAPP oligomers is largely reduced by the binding to Zn(ɪɪ) and Cu(ɪɪ) at both peptide-to-metal ratios, implying that the Zn(ɪɪ)- and Cu(ɪɪ)-

associated hIAPP oligomer species should be less disruptive to the membrane than metal-free hIAPP oligomer species, as observed in the results of the 10-peptide oligomers. Therefore, a more grievous damage of the membrane by hIAPP oligomers formed in the presence of Zn(ɪɪ) and Cu(ɪɪ) at a peptide-to-metal ratio of 1 : 1 than in the absence of the metal ions could be attributed to a significant increase in the quantity of hIAPP oligomers promoted by the binding of Zn(ɪɪ) and Cu(ɪɪ) to hIAPP at this relatively high concentration of metal ions. Although the ability of Zn(ɪɪ)- or Cu(ɪɪ)-associated hIAPP oligomer species to disrupt the membrane of POPC/POPG 4 : 1 LUVs is smaller than that of metal-free hIAPP oligomer species for an individual oligomer, the total amount of hIAPP oligomers involving in the membrane disruption in the presence of the metal ions at a peptide-to-metal ratio of 1 : 1 could be much larger than that of hIAPP oligomers formed in the absence of the metal ions. The role played by a great increase in the amount of oligomers in the membrane damage could be larger than that played by a decrease in the ability of the oligomers to disrupt the membrane at a peptide-to-metal ratio of 1 : 1. In contrast, the quantity of hIAPP oligomers formed in the presence of Zn(ɪɪ) or Cu(ɪɪ) could not be increased significantly relative to that of the oligomers formed in the absence of the metal ions at a peptide-to-metal ratio of 1 : 0.33. In this situation, the difference between metal-associated oligomers and metal-free oligomers in the membrane damage could be mainly determined by the difference in the ability of the oligomer individuals to damage the membrane, and therefore a less membrane damage is observed in the presence of Zn(ɪɪ) and Cu(ɪɪ) at a peptide-to-metal ratio of 1 : 0.33 than in the absence of the metal ions. IAPP is known to change its conformation during the evolution of the aggregates, and this changes its affinity to lipid membranes.[65] Therefore, there is another possibility that the difference in the conformation change of hIAPP at a low (1 : 0.33) or a higher (1 : 1) concentration of Cu(ɪɪ) or Zn(ɪɪ) leads to the difference in the membrane leakage at the two concentrations of metal ions. However, this possibility can be excluded by the CD results which show that Cu-associated hIAPP (or Zn-associated hIAPP) undergoes similar process of conformation change at the two concentrations of metal ions and the rate in the conformation change of hIAPP is decreased by the binding of the metal ions either at a low (1 : 0.33) or a higher (1 : 1) concentration of metal ions. A little bit stronger inhibition of the membrane damage by hIAPP oligomers formed in the presence of Cu(ɪɪ) than in the presence of Zn(ɪɪ) at a peptide-to-metal ratio of 1 : 0.33 could originate from a more compact packing of Cu(ɪɪ)-associated hIAPP oligomers than Zn(ɪɪ)-associated hIAPP oligomers,[42] while a slightly larger enhancement in the membrane damage activity of hIAPP oligomers in the presence of Cu(ɪɪ) than in the presence of Zn(ɪɪ) at a peptide-to-metal ratio of 1 : 1 could originate from more abundant oligomers formed in the presence of Cu(ɪɪ) than in the presence of Zn(ɪɪ). The effects of Ca(ɪɪ) on the aggregation of hIAPP oligomers and their abilities to disrupt the lipid membrane are much smaller than those of Cu(ɪɪ) and Zn(ɪɪ) at both peptide-to-metal ratios of 1 : 0.33 and 1 : 1, likely due to a low affinity of Ca(ɪɪ) for hIAPP oligomers.

It is noted that there could be differences between the full length hIAPP and the model peptide fragment in the binding site and the residues involved in the coordination with metal ions. Although we did not obtain the information on the binding site and binding affinity, we found that the binding of both hIAPP and its fragment with the metal ions decreases the hydrophobic exposure of the peptide oligomers. This is a common feature of these peptide/metal oligomers. In this point, the effect of the metal ions on the oligomeric feature of either peptide fragment or full-length peptide is the same, whatever peptide–metal binding patterns are.

Conclusions

The studies on both the short peptide hIAPP18-27 and the full-length hIAPP confirm that the surface hydrophobicity of the oligomers and the ability of the oligomers to disrupt the membrane are reduced by the binding of the oligomers to divalent metal ions of calcium, zinc and copper. However, the membrane disruption is either reduced or enhanced by the binding of hIAPP oligomers to Zn(II) and Cu(II), depending on the proportion of peptide to metal ion. The difference in the observed membrane disruption at different peptide-to-metal ratios is attributed to a competition between an increase in the abundance of metal-associated hIAPP oligomer species and a decrease in its disruptive ability. The total enhancement effect generated by the increase in the quantity of hIAPP oligomers in the membrane damage could prevail over the total inhibition effect generated by the decrease in the ability of oligomer individuals at a peptide-to-metal ratio of 1 : 1, while the situation could be reversed at a peptide-to-metal ratio of 1 : 0.33.

Experimental section

Materials

Peptides were synthesized by Shanghai Science Peptide Biological Technology Co. Ltd. (Shanghai, China) with a purity of >98% that was verified by mass spectroscopy and high-performance liquid chromatography. Lipids POPC (1-palmitoyl-2-oleoyl-sn-glycero-3-phosphocholine) and POPG (1-palmitoyl-2-oleoyl-sn-glycero-3-phospho-(1′-rac-glycerol)) were purchased from Avanti Polar Lipids, Inc. (Alabaster, AL). HFIP (1,1,1,3,3,3-hexafluoroisopropanol), $ZnCl_2$, $CuCl_2 \cdot 2H_2O$, $CaCl_2$, and other chemical reagents were purchased from Sigma-Aldrich (St. Louis., MO).

Pretreatment of peptides

Synthesized peptide powder was dissolved in HFIP at a concentration of 1 mg mL^{-1} and shaken on a mixer for several seconds so that the powdered peptide can be fully dissolved. The peptide/HFIP solution was sonicated by water-bath for 1 hour at a temperature below 25 °C to disrupt the pre-existing aggregates. The sample was then frozen in liquid nitrogen for 30 minutes and freeze-dried in a freeze dryer for about 12 hours.

Preparation of 10-peptide oligomers

The freeze-dried 10-peptide powder was either hydrated in 100 μL Milli-Q water or hydrated in 100 μL Milli-Q water containing salt (each of $ZnCl_2$, $CuCl_2 \cdot 2H_2O$ or $CaCl_2$) at 4 °C, keeping the concentrations of peptide and metal ion at 1 mM each, i.e., a molar ratio of peptide to metal ion at 1 : 1. The short peptide oligomers were obtained by incubating peptide alone or the mixture of peptide with metal ion in 4 °C Milli-Q water for 10 minutes. The final pH values of the solutions were 3.90, 3.87, 3.88 and 3.65 for ia10, ia10/Ca, ia10/Zn and ia10/Cu, respectively.

Preparation of large unilamellar vesicles (LUVs)

A certain amount of POPC and POPG with a molar ratio of 4 : 1 was dissolved in a mixed solvent of chloroform/methanol (2 : 1 v/v). After vortex for 10 minutes, the mixed solvent was blow-dried by a stream of nitrogen. The resulting film was further dried in a vacuum dryer overnight to remove residual organic solvents. The dry lipid film was hydrated in 25 mM phosphate buffer containing 50 mM NaCl (or 50 mM NaF for CD experiment, or 50 mM NaCl and 70 mM calcein for leakage assay) at pH 7.4. After incubation for 1 h at room temperature, the solution was freeze-thawed ten cycles and extruded 20 times through a polycarbonate filter (0.1 μm pore size). The LUVs encapsulating calcein were dialyzed for three days at room temperature through a membrane with a cut-off of 2000 Da to eliminate any dye not encapsulated into the LUVs.

Sample preparation

Preparation of 10-peptide oligomer samples: a certain volume of oligomer stock solution prepared in 4 °C Milli-Q water at a peptide concentration of 1 mM was added in LUV-free or LUV suspended phosphate buffer with 50 mM NaCl (or NaF for the CD experiments) at pH 7.4 at desired concentrations of peptide and lipid. Preparation of hIAPP samples: a certain volume of hIAPP stock solution prepared in 4 °C Milli-Q water at a concentration of 1 mM was added in LUV-free or LUV suspended phosphate buffer with 50 mM NaCl or NaF at pH 7.4 at desired concentrations of peptide and lipid, or a certain volume of hIAPP stock solution was mixed with a small volume of phosphate buffer dissolving metal ions in advance and then the mixture was added in LUV-free or LUV suspended phosphate buffer with 50 mM NaCl or NaF at pH 7.4 at desired concentrations of peptide and lipid. Thioflavin-T (ThT) was added in buffer solution in advance for the ThT fluorescence assays and the concentration of ThT was 20 μM in the final sample solutions. A stock solution of ANS (1-anilino-naphthalene-8-sulfonate) at a concentration of 5 mM was prepared in 4 °C Milli-Q water for the ANS binding fluorescence experiments.

Fluorescent dye leakage assay

The leakage assays were performed on a RF-5301 PC spectrophotometer (Shimadzu, Japan) at room temperature using calcein as a probe. The fluorescence was excited at 495 nm and the emission at 562 nm was monitored. The fluorescence signals

were collected after an average of three scans and the percentages of the dye leakage were obtained by the following equation:

$$\% \text{ of leakage} = (F - F_{\text{baseline}})/(F_{\max} - F_{\text{baseline}}) \times 100\% \quad (1)$$

where F and F_{baseline} are the fluorescence intensity observed in the presence and absence of peptide, respectively. $F_{\max}$ represents the fluorescence intensity for the 100% leakage of calcein. It was obtained by the addition of 0.2% Triton-X in the sample solution.

Transmission electron microscopy

Oligomer stock solution with a peptide concentration of 1 mM prepared at 4 °C was diluted by Milli-Q water to 25 μM. A volume of 10 μL of the solution was deposited onto a 300-mesh Formvar/carboncoated copper grid at 4 °C for 5 minutes. After that, it was washed twice with 10 μL Milli-Q water, and the excess solution was removed with filter paper. Finally, the sample was air-dried overnight for testing. Transmission electron microscopy (TEM) images were observed under a transmission electron microscope (JEM-2100F, JEOL Co., Ltd., Japan) operating at an accelerating voltage of 200 kV. The diameters of 100 randomly selected oligomers were measured using Nano Measurer software and the mean diameter and SD value were calculated based on the diameter distributions.

Dynamic light scattering measurements

Peptide or oligomer stock solution was diluted by Milli-Q water to 5 μM. Milli-Q water was filtered with a 0.22 μm filter to prevent the influence of impurities on experimental data. Dynamic light scattering (DLS) measurements were carried out using Zetasizer Nano ZS instrument (Malven Instruments, UK) at room temperature. Intensity of scattered light was detected at an angle of 90° and hydrodynamic diameter of sample was calculated using Zetasizer Nano software. Each sample was measured ten times and the results were expressed as the average value.

Far-UV circular dichroism spectroscopy

Far-UV circular dichroism (Far-UV CD) spectra were recorded on a Chirascan-Plus instrument (Applied Photophysics Ltd, UK) at room temperature under a constant flow of nitrogen gas. A quartz cuvette of 1 mm pathlength was used. The spectra were scanned from 190 nm to 260 nm three times. The background spectra were recorded separately and subtracted from the spectra of the samples.

Thioflavin-T fluorescence assay

The ThT fluorescence assays were performed immediately after the sample preparation using a RF-5301 PC spectrofluorophotometer (Shimadzu, Japan) at room temperature without shaking. The emission spectra were scanned in the range of 400–600 nm at an excitation wavelength of 440 nm and an emission at 482 nm was measured. All experiments were repeated three times by separately prepared samples.

Atomic force microscopy

A volume of 5 μL sample solution via different times of incubation was deposited onto a freshly cleaved mica surface for 15 minutes. Then, the sample on mica was washed twice with either Milli-Q water (for all oligomer samples) or phosphate buffer (for all hIAPP samples) and baked for 5 minutes at 65 °C in an oven to flat the lipid film. Atomic force microscopy (AFM) measurements were performed at room temperature on a Fast Scan AFM instrument (Bruker Instruments Inc., German) using tapping mode. Images were collected at a scan rate of 1 Hz and a scan angle of 0°.

Acrylamide fluorescence quenching experiment

The phenylalanine fluorescence spectra were recorded on a RF-5301 PC spectrofluorophotometer (Shimadzu, Japan) with an excitation wavelength of 256 nm after the addition of certain quantity of acrylamide stock solution (5 M) to freshly prepared oligomer sample solution at 4 °C. Each emission spectrum was scanned from 270 nm to 340 nm for three times and the results were averaged.

The degree of fluorescence quenching was estimated by K_{sv}, a quenching constant obtained from the Stern–Volmer equation:

$$F_0/F = 1 + K_{\text{sv}}[Q] \quad (2)$$

where F_0 and F are the fluorescence intensities in the absence and presence of the quencher, respectively, and [Q] is the concentration of quencher.

ANS binding assay

ANS binding assays were performed on a RF-5301 PC spectrophotometer (Shimadzu, Japan) with an excitation of 355 nm. The fluorescence emission between 400 nm and 650 nm was measured. The stock solution of 10-peptide oligomer or hIAPP in 4 °C Milli-Q water was diluted using 4 °C Milli-Q water to a desired concentration and the ANS stock solution was added in the sample solution at a desired concentration.

Conflicts of interest

There are no conflicts of interest to declare.

Acknowledgements

Notes and references

1 L. Marzban, G. Trigo-Gonzalez and C. B. Verchere, *Mol. Endocrinol.*, 2005, **19**, 2154–2163.
2 P. Westermark, A. Andersson and G. T. Westermark, *Physiol. Rev.*, 2011, **91**, 795–826.
3 A. N. Roberts, B. Leighton, J. A. Todd, D. Cockburn, P. N. Schofield, R. Sutton, S. Holt, Y. Boyd, A. J. Day,

E. A. Foot, A. C. Willis, K. B. M. Reid and G. J. S. Cooper, *Proc. Natl. Acad. Sci. U. S. A.*, 1989, **86**, 9662–9666.

4 E. T. A. S. Jaikaran and A. Clark, *Biochim. Biophys. Acta, Mol. Basis Dis.*, 2001, **1537**, 179–203.

5 L. Marzban, K. Park and C. B. Verchere, *Exp. Gerontol.*, 2003, **38**, 347–351.

6 A. Abedini and A. M. Schmidt, *FEBS Lett.*, 2013, **587**, 1119–1127.

7 C. M. Dobson, *Protein Pept. Lett.*, 2006, **13**, 219–227.

8 C. Soto, *Nat. Rev. Neurosci.*, 2003, **4**, 49–60.

9 E. N. Cline, M. A. Bicca, K. L. Viola and W. L. Klein, *J. Alzheimer's Dis.*, 2018, **64**, S567–S610.

10 M. Ingelsson, *Front. Neurosci.*, 2016, **10**, 408.

11 J. R. Brender, S. Salamekh and A. Ramamoorthy, *Acc. Chem. Res.*, 2012, **45**, 454–462.

12 K. Weise, D. Radovan, A. Gohlke, N. Opitz and R. Winter, *ChemBioChem*, 2010, **11**, 1280–1290.

13 Y. Bram, A. Frydman-Marom, I. Yanai, S. Gilead, R. Shaltiel-Karyo, N. Amdursky and E. Gazit, *Sci. Rep.*, 2014, **4**, 4267.

14 H.-L. Zhao, Y. Sui, J. Guan, L. He, X.-M. Gu, H. K. Wong, L. Baum, F. M. M. Lai, P. C. Y. Tong and J. C. N. Chan, *Transl. Res.*, 2009, **153**, 24–32.

15 M. F. M. Engel, L. Khemtémourian, C. C. Kleijer, H. J. D. Meeldijk, J. Jacobs, A. J. Verkleij, B. d. Kruijff, J. A. Killian and J. W. M. Höppener, *Proc. Natl. Acad. Sci. U. S. A.*, 2008, **105**, 6033–6038.

16 J. D. Green, L. Kreplak, C. Goldsbury, X. Li Blatter, M. Stolz, G. S. Cooper, A. Seelig, J. Kistler and U. Aebi, *J. Mol. Biol.*, 2004, **342**, 877–887.

17 M. Anguiano, R. J. Nowak and P. T. Lansbury, *Biochemistry*, 2002, **41**, 11338–11343.

18 M. F. Tomasello, A. Sinopoli and G. Pappalardo, *J. Diabetes Res.*, 2015, **2015**, 918573.

19 M. Rowińska-Żyrek, *Dalton Trans.*, 2016, **45**, 8099–8106.

20 A. Magrì, D. La Mendola, V. G. Nicoletti, G. Pappalardo and E. Rizzarelli, *Chem. - Eur. J.*, 2016, **22**, 13287–13300.

21 K. Lemaire, M. A. Ravier, A. Schraenen, J. W. M. Creemers, R. Van de Plas, M. Granvik, L. Van Lommel, E. Waelkens, F. Chimienti, G. A. Rutter, P. Gilon, P. A. in't Veld and F. C. Schuit, *Proc. Natl. Acad. Sci. U. S. A.*, 2009, **106**, 14872–14877.

22 J. R. Brender, J. Krishnamoorthy, G. M. Messina, A. Deb, S. Vivekanandan, C. La Rosa, J. E. Penner-Hahn and A. Ramamoorthy, *Chem. Commun.*, 2013, **49**, 3339–3341.

23 P. Nedumpully-Govindan and F. Ding, *Sci. Rep.*, 2015, **5**, 8240.

24 A. B. Chausmer, *J. Am. Coll. Nutr.*, 1998, **17**, 109–115.

25 C. G. Taylor, *BioMetals*, 2005, **18**, 305–312.

26 R. Sladek, G. Rocheleau, J. Rung, C. Dina, L. Shen, D. Serre, P. Boutin, D. Vincent, A. Belisle, S. Hadjadj, B. Balkau, B. Heude, G. Charpentier, T. J. Hudson, A. Montpetit, A. V. Pshezhetsky, M. Prentki, B. I. Posner, D. J. Balding, D. Meyre, C. Polychronakos and P. Froguel, *Nature*, 2007, **445**, 881–885.

27 E. Zeggini, M. N. Weedon, C. M. Lindgren, T. M. Frayling, K. S. Elliott, H. Lango, N. J. Timpson, J. R. B. Perry, N. W. Rayner, R. M. Freathy, J. C. Barrett, B. Shields, A. P. Morris, S. Ellard, C. J. Groves, L. W. Harries, J. L. Marchini, K. R. Owen, B. Knight, L. R. Cardon, M. Walker, G. A. Hitman, A. D. Morris, A. S. F. Doney, The Wellcome Trust Case Control Consortium (WTCCC), M. I. McCarthy and A. T. Hattersley, *Science*, 2007, **316**, 1336–1341.

28 H. Staiger, F. Machicao, N. Stefan, O. Tschritter, C. Thamer, K. Kantartzis, S. A. Schäfer, K. Kirchhoff, A. Fritsche and H. U. Häring, *PLoS One*, 2007, **2**, e832.

29 E. D. Harris, *Exp. Biol. Med.*, 1991, **196**, 130–140.

30 A. Viktorínová, E. Tošerová, M. Križko and Z. Ďuračková, *Metabolism*, 2009, **58**, 1477–1482.

31 J. W. Eaton and M. Qian, *Mol. Cell. Biochem.*, 2002, **234**, 135–142.

32 A. H. Zargar, M. I. Bashir, A. R. Khan, S. R. Masoodi, B. A. Laway, A. I. Wani and F. A. Dar, *Exp. Clin. Endocrinol. Diabetes*, 2000, **108**, 397–400.

33 M. Kawahara, Y. Kuroda and E. R. N Arispe, *J. Biol. Chem.*, 2000, **275**, 14077–14083.

34 J. Parkash, M. A. Chaudhry, A. S. Amer, S. Christakos and W. B. Rhoten, *Endocrine*, 2002, **18**, 221–229.

35 M. Barbagallo, R. K. Gupta and L. M. Resnick, *Diabetes Care*, 1996, **19**, 1393–1398.

36 M. Barbagallo, S. Novo, G. Licata and L. M. Resnick, *Int. J. Angiol.*, 1993, **12**, 365–370.

37 S. Salamekh, J. R. Brender, S. J. Hyung, R. P. Nanga, S. Vivekanandan, B. T. Ruotolo and A. Ramamoorthy, *J. Mol. Biol.*, 2011, **410**, 294–306.

38 J. R. Brender, K. Hartman, R. P. R. Nanga, N. Popovych, R. de la Salud Bea, S. Vivekanandan, E. N. G. Marsh and A. Ramamoorthy, *J. Am. Chem. Soc.*, 2010, **132**, 8973–8983.

39 P. Nedumpully-Govindan, Y. Yang, R. Andorfer, W. Cao and F. Ding, *Biochemistry*, 2015, **54**, 7335–7344.

40 V. Wineman-Fisher and Y. Miller, *Phys. Chem. Chem. Phys.*, 2016, **18**, 21590–21599.

41 J. Flannick, G. Thorleifsson, N. L. Beer, S. B. Jacobs, N. Grarup, N. P. Burtt, A. Mahajan, C. Fuchsberger, G. Atzmon, R. Benediktsson, J. Blangero, D. W. Bowden, I. Brandslund, J. Brosnan, F. Burslem, J. Chambers, Y. S. Cho, C. Christensen, D. A. Douglas, R. Duggirala, Z. Dymek, Y. Farjoun, T. Fennell, P. Fontanillas, T. Forsen, S. Gabriel, B. Glaser, D. F. Gudbjartsson, C. Hanis, T. Hansen, A. B. Hreidarsson, K. Hveem, E. Ingelsson, B. Isomaa, S. Johansson, T. Jorgensen, M. E. Jorgensen, S. Kathiresan, A. Kong, J. Kooner, J. Kravic, M. Laakso, J. Y. Lee, L. Lind, C. M. Lindgren, A. Linneberg, G. Masson, T. Meitinger, K. L. Mohlke, A. Molven, A. P. Morris, S. Potluri, R. Rauramaa, R. Ribel-Madsen, A. M. Richard, T. Rolph, V. Salomaa, A. V. Segre, H. Skarstrand, V. Steinthorsdottir, H. M. Stringham, P. Sulem, E. S. Tai, Y. Y. Teo, T. Teslovich, U. Thorsteinsdottir, J. K. Trimmer, T. Tuomi, J. Tuomilehto, F. Vaziri-Sani, B. F. Voight, J. G. Wilson, M. Boehnke, M. I. McCarthy, P. R. Njolstad, O. Pedersen, T. D. C. Go, T. D. G. Consortium, L. Groop, D. R. Cox, K. Stefansson and D. Altshuler, *Nat. Genet.*, 2014, **46**, 357–363.

42 S. J. C. Lee, T. S. Choi, J. W. Lee, H. J. Lee, D. G. Mun, S. Akashi, S. W. Lee, M. H. Lim and H. I. Kim, *Chem. Sci.*, 2016, **7**, 5398–5406.

43 B. Ward, K. Walker and C. Exley, *J. Inorg. Biochem.*, 2008, **102**, 371–375.

44 A. Masad, L. Hayes, B. J. Tabner, S. Turnbull, L. J. Cooper, N. J. Fullwood, M. J. German, F. Kametani, O. M. El-Agnaf and D. Allsop, *FEBS Lett.*, 2007, **581**, 3489–3493.

45 L. Ma, X. Li, Y. Wang, W. Zheng and T. Chen, *J. Inorg. Biochem.*, 2014, **140**, 143–152.

46 A. Sinopoli, A. Magrì, D. Milardi, M. Pappalardo, P. Pucci, A. Flagiello, J. J. Titman, V. G. Nicoletti, G. Caruso, G. Pappalardo and G. Grasso, *Metallomics*, 2014, **6**, 1841–1852.

47 E. C. Lee, E. Ha, S. Singh, L. Legesse, S. Ahmad, E. Karnaukhova, R. P. Donaldson and A. M. Jeremic, *Phys. Chem. Chem. Phys.*, 2013, **15**, 12558–12571.

48 E. Atrian-Blasco, P. Gonzalez, A. Santoro, B. Alies, P. Faller and C. Hureau, *Coord. Chem. Rev.*, 2018, **371**, 38–55.

49 M. F. M. Sciacca, D. Milardi, G. M. L. Messina, G. Marletta, J. R. Brender, A. Ramamoorthy and C. La Rosa, *Biophys. J.*, 2013, **104**, 173–184.

50 M. F. M Sciacca, M. Pappalardo, D. Milardi, D. M. Grasso and C. La Rosa, *Arch. Biochem. Biophys.*, 2008, **477**, 291–298.

51 M. Bucciantini, G. Calloni, F. Chiti, L. Formigli, D. Nosi, C. M. Dobson and M. Stefani, *J. Biol. Chem.*, 2004, **279**, 31374–31382.

52 A. Demuro, E. Mina, R. Kayed, S. C. Milton, I. Parker and C. G. Glabe, *J. Biol. Chem.*, 2005, **280**, 17294–17300.

53 R. Kayed, E. Head, J. L. Thompson, T. M. McIntire, S. C. Milton, C. W. Cotman and C. G. Glabe, *Science*, 2003, **300**, 486–489.

54 J. T. Nielsen, M. Bjerring, M. D. Jeppesen, R. O. Pedersen, J. M. Pedersen, K. L. Hein, T. Vosegaard, T. Skrydstrup, D. E. Otzen and N. C. Nielsen, *Angew. Chem., Int. Ed.*, 2009, **48**, 2118–2121.

55 H. F. Christoffersen, M. Andreasen, S. Zhang, E. H. Nielsen, G. Christiansen, M. Dong, T. Skrydstrup and D. E. Otzen, *Biochim. Biophys. Acta, Biomembr.*, 2015, **1854**, 1890–1897.

56 J. R. Brender, D. L. Heyl, S. Samisetti, S. A. Kotler, J. M. Osborne, R. R. Pesaru and A. Ramamoorthy, *Phys. Chem. Chem. Phys.*, 2013, **15**, 8908–8915.

57 J. R. Brender, U. H. N. Durr, D. Heyl, M. B. Budarapu and A. Ramamoorthy, *Biochim. Biophys. Acta, Biomembr.*, 2007, **1768**, 2026–2029.

58 Y. Wei, J. Lu, T. Lu, F. Meng, J. Xu, L. Wang, Y. Li, L. Wang and F. Li, *Phys. Chem. Chem. Phys.*, 2016, **18**, 29847–29857.

59 S. Wang, F. Meng, R. Hao, C. Wang and F. Li, *Biochim. Biophys. Acta, Biomembr.*, 2020, **1862**, 183108.

60 C. Sánchez-López, R. Cortés-Mejía, M. C. Miotto, A. Binolfi, C. O. Fernández, J. M. Del Campo and L. Quintanar, *Inorg. Chem.*, 2016, **55**, 10727–10740.

61 B. Mannini, E. Mulvihill, C. Sgromo, R. Cascella, R. Khodarahmi, M. Ramazzotti, C. M. Dobson, C. Cecchi and F. Chiti, *ACS Chem. Biol.*, 2014, **9**, 2309–2317.

62 S. Campioni, B. Mannini, M. Zampagni, A. Pensalfini, C. Parrini, E. Evangelisti, A. Relini, M. Stefani, C. M. Dobson, C. Cecchi and F. Chiti, *Nat. Chem. Biol.*, 2010, **6**, 140–147.

63 B. Bolognesi, J. R. Kumita, T. P. Barros, E. K. Esbjorner, L. M. Luheshi, D. C. Crowther, M. R. Wilson, C. M. Dobson, G. Favrin and J. J. Yerbury, *ACS Chem. Biol.*, 2010, **5**, 735–740.

64 L. Rivillas-Acevedo, C. Sánchez-López, C. Amero and L. Quintanar, *Inorg. Chem.*, 2015, **54**, 3788–3796.

65 A. Rawat, B. K. Maity, B. Chandra and S. Maiti, *Biochim. Biophys. Acta, Biomembr.*, 2018, **1860**, 1734–1740.